Mem. Fac. Eng., Osaka City Univ., Vol. 38, pp.27—37(1997)

Tangent Stiffness Equations for Laterally Distributed Loaded Member

Yoshiya TANIGUCHI*, Toshitsugu SAKA** and Hideto TANAKA***
(Received September 30, 1997)

Synopsis

Tangent stiffness equations for a beam-column which is subjected to either uniformly or sinusoidally distributed lateral load are presented. The equations have been derived by differentiating the slope-deflection equations under axial forces for a member. Then, the tangent stiffness equations take into account axial forces, a bowing effect and laterally distributed loads. Elastic buckling behavior of parallel chord latticed beams with laterally distributed loads is investigated, to compare the results of the present method with a conventional method in which the distributed loads are considered as concentrated loads at additional nodes of a member. Furthermore, buckling tests were carried out to confirm the derived equations and to make clear the buckling behavior of space frame structures. As a result, the new equations can lead to a good efficiency of estimating equilibrium paths and a significant savings in the core storage and computing time required for the analysis of space frame structures.

KEYWORDS: Tangent stiffness, lateral load, distributed load

Introduction

In treating a frame structure which is subjected to a distributed load, an ordinary method is a so-called conventional matrix method that divides a two-nodded beam-column element into finite segments and considers a distributed load as concentrated loads acting on additional nodes of the element. However, for space frame structures with the great number of members, the advantage of the preceding approximation with respect to loads can lead to a considerable increase in the number of degrees of freedom and in the computing time. It may be, therefore, desirable to use member force-deformation equations considering laterally distributed loads. In the literature, slope-deflection equations under axial forces for a member that is subjected to either uniformly or sinusoidally distributed lateral loads have been already presented [1),2)]. However, tangent stiffness expressions are necessary for space frame structures to study the effect of distributed loads on constituent members, since the flexural rigidity of members is very different from that of a whole structural system.

Space frame structures are widely used to cover large areas without the need for intermediate supports. The two main components of any space frame structure are members and joints. In design, it is generally assumed that only joints are directly subjected to external loads. The constituent members transmit the loads from a joint to the other joint as axial forces. However if the possibility of a larger space frame structural system may be pursued in the future, the existing structural system must be changed, barring unexpected developments of materials. Then, one of developed structural systems is the hybrid system that combines a space frame structure with a cladding, for example, a concrete slab, steel panels or membrane, etc. In such a case, constituent members may be directly subjected to external loads. From this viewpoints, tangent stiffness equations for uniformly or sinusoidally distributed laterally loaded members under axial forces are presented. As a numerical example, the load-deflection relationships and buckling loads are estimated for parallel chord latticed beam and the results by the present method are compared with a conventional matrix method, in which distributed loads are assumed to be concentrated ones. Furthermore, buckling tests were carried out to confirm the derived equations and to make clear the buckling behavior of space frame structures subjected to laterally distributed loads.

Member Force-Deformation Relations

Relative deformations and forces of the member subjected to laterally distributed loads are shown in Fig.1.

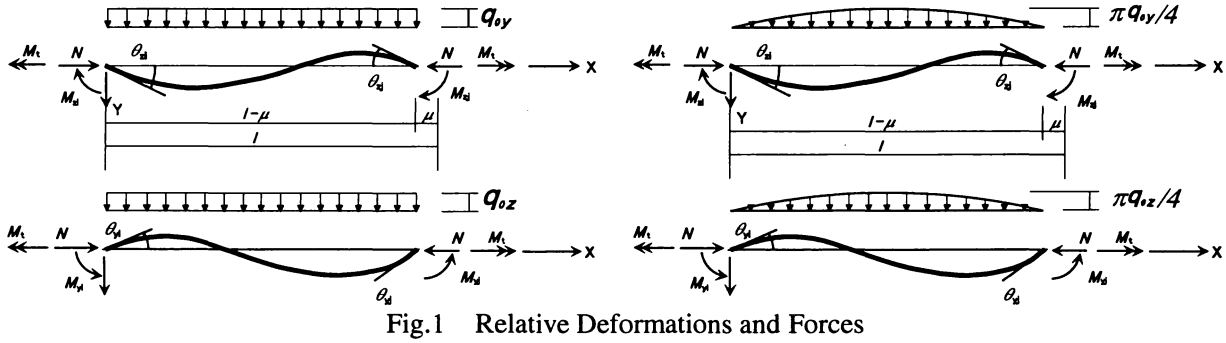

Fig.1 Relative Deformations and Forces

* Research Associate, Department of Architecture and Building Engineering
** Professor, Department of Architecture and Building Engineering
*** Engineer, Takenaka Corporation, Osaka

The member is assumed to be an elastic straight one whose section is uniform and biaxial symmetric. The shear deformation of a member is neglected. The relation between the member forces$\{s\}$ and deformations$\{u\}$ is defined as follows.

$$\{s\}=[k]\{u\}+\{r\} \tag{1}$$

in which $\{s\}=[M_{yi}\ M_{yj}\ M_{zi}\ M_{zj}\ M_T\ N]^T$, $\{u\}=[\theta_{yi}\ \theta_{yj}\ \theta_{zi}\ \theta_{zj}\ \theta_T\ \mu-(\mu_y+\mu_z)]^T$ and $\{r\}=[r_y\ -r_y\ -r_z\ r_z\ 0\ 0]^T$. $[k]$ is an elastic stiffness matrix for a beam-column and given by

$$[k]=\frac{EI}{l}\begin{bmatrix} c_y\alpha_y & c_y\beta_y & 0 & 0 & 0 & 0 \\ c_y\beta_y & c_y\alpha_y & 0 & 0 & 0 & 0 \\ 0 & 0 & c_z\alpha_z & c_z\beta_z & 0 & 0 \\ 0 & 0 & c_z\beta_z & c_z\alpha_z & 0 & 0 \\ 0 & 0 & 0 & 0 & \dfrac{GJ-r_0^2N}{EI} & 0 \\ 0 & 0 & 0 & 0 & 0 & \dfrac{EA}{EI} \end{bmatrix} \tag{2}$$

in which α and β = stability functions[3], EI = a standard flexural rigidity, GJ = a torsional rigidity and EA = an extensional rigidity. The coefficients c_y, c_z and r_0^2 are shown in (3.a-c).

$$c_y=\frac{EI_y}{EI},\quad c_z=\frac{EI_z}{EI},\quad r_0^2=\frac{EI_y+EI_z}{EA} \tag{3.a-c}$$

The subscripts y, z denote the each term with respect to y axis and z axis, respectively. The loading term r_y, r_z in (1) are given as the following expressions, in which the subscripts u, s mean the each term for the uniformly and sinusoidally distributed load, respectively. The loading term r_{uy} of a uniformly distributed load is given by

$$r_{uy}=\frac{2q_{ny}\pi EI_y\varepsilon_y(\alpha_y-\beta_y)}{l} \tag{4}$$

in which ε_y is given as Table 1.

Table 1 The functions of ε_y

N	ε_y
$N>0$	$\dfrac{2\left\{1-\cos\left(\pi\sqrt{P_{ny}}\right)\right\}-\pi\sqrt{P_{ny}}\sin\left(\pi\sqrt{P_{ny}}\right)}{\pi P_{ny}\sqrt{P_{ny}}\sin\left(\pi\sqrt{P_{ny}}\right)}$
$N=0$	$\dfrac{\pi^2}{12}$
$N<0$	$\dfrac{2\left\{\cosh\left(\pi\sqrt{\lvert P_{ny}\rvert}\right)-1\right\}-\pi\sqrt{\lvert P_{ny}\rvert}\sinh\left(\pi\sqrt{\lvert P_{ny}\rvert}\right)}{\pi P_{ny}\sqrt{\lvert P_{ny}\rvert}\sinh\left(\pi\sqrt{\lvert P_{ny}\rvert}\right)}$

The loading term r_s of a sinusoidally distributed is given by

$$r_{sy}=\frac{q_{ny}\pi EI_y(\alpha_y-\beta_y)}{l(1-P_{ny})} \tag{5}$$

$$r_{sy}=\frac{q_{ny}\pi^3 EI_y}{4l}\quad \text{at}\quad P_{ny}=1 \tag{6}$$

In the above expressions, P_{ny}, q_{ny} are given by

$$P_{ny} = \frac{Nl^2}{\pi^2 EI_y}, \qquad q_{ny} = \frac{q_{0z} l^3}{4\pi^3 EI_y} \tag{7, 8}$$

All the subscript y can be replaced by z. The functions μ_y and μ_z in (1), which are length correction factor due to bowing effect, are shown as follows.

$$\frac{\mu_y}{l} = b_{y1}(\theta_{yi} + \theta_{yj})^2 + b_{y2}(\theta_{yi} - \theta_{yj})^2 - b_{y3}(\theta_{yi} - \theta_{yj}) + b_{y4} \tag{9}$$

$$\frac{\mu_z}{l} = b_{z1}(\theta_{zi} + \theta_{zj})^2 + b_{z2}(\theta_{zi} - \theta_{zj})^2 + b_{z3}(\theta_{zi} - \theta_{zj}) + b_{z4} \tag{10}$$

in which b_{y1} and b_{y2} are bowing functions [4] , and b_{y3} and b_{y4} are new bowing functions resulting from the laterally distributed loads and given by (11)-(14). The functions of the uniformly distributed load are given by (11) and (12), and those of the sinusoidally distributed loads are given by (13) and (14).

$$b_{uy3} = \frac{4\pi q_{ny}}{P_{ny}} \left\{ 2b_{y2} - \frac{1}{2(\alpha_y + \beta_y)} \right\}, \quad b_{uy3} = \pi^3 q_{ny} / 180 \quad \text{at } P_{ny} = 0 \tag{11}$$

$$b_{uy4} = \left(\frac{4\pi q_{ny}}{P_{ny}} \right)^2 \left\{ b_{y2} - \frac{1}{2(\alpha_y + \beta_y)} + \frac{1}{24} \right\}, \quad b_{uy4} = \pi^6 q_{ny}^2 / 3780 \quad \text{at } P_{ny} = 0 \tag{12}$$

$$b_{sy3} = \frac{q_{ny}}{\pi(1 - P_{ny})} \left\{ \frac{\alpha_y - \beta_y}{1 - P_{ny}} - 4\pi^2 b_{y2} \right\}, \quad b_{sy3} = \pi q_{ny} / 16 \quad \text{at } P_{ny} = 1 \tag{13}$$

$$b_{sy4} = \left(\frac{q_{ny}}{1 - P_{ny}} \right)^2 \left\{ \frac{\pi^2}{4} + 4\pi^2 b_{y2} - \frac{2(\alpha_y - \beta_y)}{1 - P_{ny}} \right\}, \quad b_{sy4} = \pi^2(\pi^2 - 6) q_{ny}^2 / 192 \quad \text{at } P_{ny} = 1 \tag{14}$$

Tangent Stiffness Equations of Member

The incremental vectors of member forces, relative deformations and loading terms are denoted as $\{\Delta s\}$,$\{\Delta u\}$ and $\{\Delta r\}$, respectively. The relation between the incremental vectors can be written as

$$\{\Delta s\} = [\Delta k]\{\Delta u\} + \{\Delta r\} \tag{15}$$

in which

$\{\Delta s\} = [\Delta M_{yi} \ \Delta M_{yj} \ \Delta M_{zi} \ \Delta M_{zj} \ \Delta M_T \ \Delta N]^T$,

$\{\Delta u\} = [\Delta \theta_{yi} \ \Delta \theta_{yj} \ \Delta \theta_{zi} \ \Delta \theta_{zj} \ \Delta \theta_T \ \Delta \mu]^T$,

$\{\Delta r\} = [\Delta r_y \ \ -\Delta r_y \ \ -\Delta r_z \ \ \Delta r_z \ \ 0 \ \ 0]^T$

and $[\Delta k]$ = an elastic tangent stiffness matrix with

$$\Delta k_{ij} = \frac{\partial s_i}{\partial u_j} + \frac{\partial s_i}{\partial N} \frac{\partial N}{\partial u_j}, \quad (i, j = 1 - 6) \tag{16}$$

The components of the tangent stiffness matrix $[\Delta k]$ are obtained as follows.

$$\Delta k_{11} = \frac{EI}{l} \left(c_y \alpha_y + \frac{G_{yi}^2}{\pi^2 H} \right), \quad \Delta k_{22} = \frac{EI}{l} \left(c_y \alpha_y + \frac{G_{yj}^2}{\pi^2 H} \right) \tag{17,18}$$

$$\Delta k_{33} = \frac{EI}{l} \left(c_z \alpha_z + \frac{G_{zi}^2}{\pi^2 H} \right), \quad \Delta k_{44} = \frac{EI}{l} \left(c_z \alpha_z + \frac{G_{zj}^2}{\pi^2 H} \right) \tag{19,20}$$

$$\Delta k_{12} = \Delta k_{21} = \frac{EI}{l} \left(c_y \beta_y + \frac{G_{yi} G_{yj}}{\pi^2 H} \right) \tag{21}$$

$$\Delta k_{34} = \Delta k_{43} = \frac{EI}{l}\left(c_z \beta_z + \frac{G_{zi} G_{zj}}{\pi^2 H} \right) \tag{22}$$

$$\Delta k_{55} = \frac{GJ - r_0^2 N}{l}, \quad \Delta k_{16} = \Delta k_{61} = \frac{G_{yi} EI}{Hl^2} \tag{23,24}$$

$$\Delta k_{26} = \Delta k_{62} = \frac{G_{yj} EI}{Hl^2}, \quad \Delta k_{36} = \Delta k_{63} = \frac{G_{zi} EI}{Hl^2} \tag{25,26}$$

$$\Delta k_{46} = \Delta k_{64} = \frac{G_{zj} EI}{Hl^2}, \quad \Delta k_{66} = \frac{\pi^2 EI}{Hl^3} \tag{27,28}$$

where

$$G_{yi} = \alpha_y' \theta_{yi} + \beta_y' \theta_{yj} + \pi^2 b_{y3}, \quad G_{yj} = \beta_y' \theta_{yi} + \alpha_y' \theta_{yj} - \pi^2 b_{y3} \tag{29,30}$$

$$G_{zi} = \alpha_z' \theta_{zi} + \beta_z' \theta_{zj} - \pi^2 b_{z3}, \quad G_{zj} = \beta_z' \theta_{zi} + \alpha_z' \theta_{zj} + \pi^2 b_{z3} \tag{31,32}$$

and

$$H = \frac{\pi^2}{\lambda^2} + \frac{\gamma_y}{c_y} + \frac{\gamma_z}{c_z}, \quad \lambda^2 = \frac{l^2 EA}{EI}, \tag{33,34}$$

$$\gamma_y = b_{y1}' (\theta_{yi} + \theta_{yj})^2 + b_{y2}' (\theta_{yi} - \theta_{yj})^2 - b_{y3}' (\theta_{yi} - \theta_{yj}) + b_{y4}' \tag{35}$$

$$\gamma_z = b_{z1}' (\theta_{zi} + \theta_{zj})^2 + b_{z2}' (\theta_{zi} - \theta_{zj})^2 + b_{z3}' (\theta_{zi} - \theta_{zj}) + b_{z4}' \tag{36}$$

in which a prime superscript indicates one differentiation with respect to P_{ny} or P_{nz}. The other components of matrix $[\Delta k]$ are zero. The functions α'_y, β'_y, b'_{y1} and b'_{y2} are listed in the reference [5]. The functions b'_{y3} and b'_{y4} are the new terms resulting from the laterally distributed loads, and given by

$$b_{uy3}' = \frac{4\pi q_{ny}}{P_{ny}} \left\{ 2b_{y2}' - \frac{2\pi^2 b_{y1}}{(\alpha_y + \beta_y)^2} - \frac{1}{P_{ny}} \left(2b_{y2} - \frac{1}{2(\alpha_y + \beta_y)} \right) \right\} \tag{37}$$

$$b_{uy3}' = \pi^5 q_{ny} / 3780 \qquad \text{at } P_{ny} = 0 \tag{38}$$

$$b_{uy4}' = \left(\frac{4\pi q_{ny}}{P_{ny}} \right)^2 \left\{ b_{y2}' - \frac{2\pi^2 b_{y1}}{(\alpha_y + \beta_y)^2} - \frac{1}{P_{ny}} \left(2b_{y2} - \frac{1}{(\alpha_y + \beta_y)} + \frac{1}{12} \right) \right\} \tag{39}$$

$$b_{uy4}' = \pi^8 q_{ny}^2 / 75600 \qquad \text{at } P_{ny} = 0 \tag{40}$$

$$b_{sy3}' = \frac{q_{ny}}{\pi(1 - P_{ny})} \left\{ \frac{2(\alpha_y - \beta_y)}{(1 - P_{ny})^2} - \frac{8\pi^2 b_{y2}}{1 - P_{ny}} - 4\pi^2 b_{y2}' \right\} \tag{41}$$

$$b_{sy3}' = \pi(\pi^2 - 6) q_{ny} / 96 \qquad \text{at } P_{ny} = 1 \tag{42}$$

$$b_{sy4}' = \left(\frac{q_{ny}}{1 - P_{ny}} \right)^2 \left\{ 4\pi^2 b_{y2}' + \frac{\pi^2}{1 - P_{ny}} \left(\frac{1}{2} + 16 b_{y2} \right) - \frac{6(\alpha_y - \beta_y)}{(1 - P_{ny})^2} \right\} \tag{43}$$

$$b_{sy4}' = \pi^2 (\pi^4 - 15\pi^2 + 70) q_{ny}^2 / 1536 \qquad \text{at } P_{ny} = 1 \tag{44}$$

The obtained tangent stiffness matrix is for member forces - relative deformations relations in local coordinates. The tangent stiffness matrix (12×12) of member forces – displacements relations in local coordinates can be obtained from considerations of geometry and equilibrium [5].

Numerical Examples

The tangent stiffness equations of laterally distributed loads have been developed here, previously. In this paragraph, some comparisons of the buckling behaviour of parallel chord latticed beams has been made between the predictions of the new tangent stiffness equations, and those of a conventional matrix method where each constituent member are divided into finite segments, with respect to a sinusoidally distributed load.

As numerical models, parallel chord latticed beams of 3 structural units shown in Fig.2 are treated. As a parameter, the number of structural units is 3, 10 and 16, and the 3 loading cases are adopted.

In Fig.2, NL loading type denotes vertical concentrated loads on upper nodes, DL type denotes distributed loads on upper chord members. CL loading type denotes equivalent concentrated loads on the additional nodes of members. In numerical analyses, the additional nodes of a member are 10 for a 3 structural unit beam and 5 for 10 and 16 structural unit beams. The mechanical properties of constituent members are shown in Table 2.

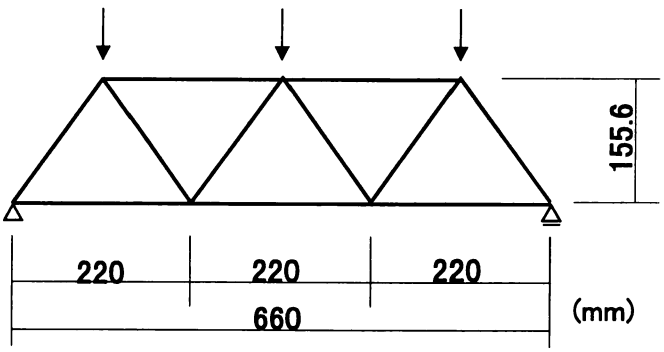

(a) NL loading type (Nodal load)

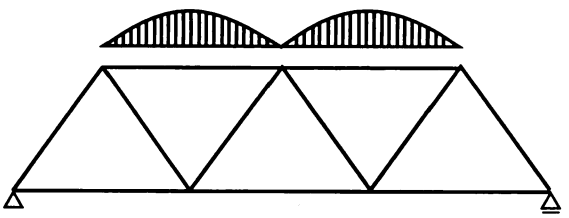

(b) DL loading type (True distributed load)

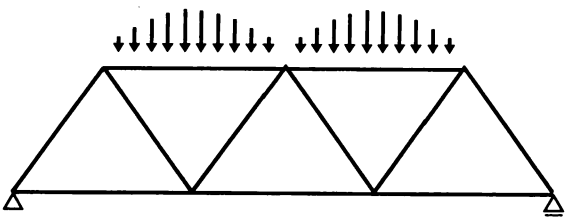

(c) CL loading type (Equivalent concentrated load on additional nodes)

Fig.2 Loading types for a parallel chord latticed beam

Table 2 Mechanical properties of members

Tubular member	Section are A	Moment inertia I
ϕ42.0×t2.0 (mm)	2.617×10^{2} (mm^2)	5.408×10^{4} (mm^4)
Young modulus E =2.145×10^{2} (kN/mm^2), Yield stress $\sigma_y = 2.354\times10^{-1}$ (kN/mm^2)		

The obtained total load-deflection relationships are shown in Figs.3, 4 and 5. The elastic buckling modes of DL and NL loading types are shown in Figs.6 and 7, respectively. In the figures, the mark▼ represents the elastic buckling load of each loading case. The mark ▽ represents the initial yield load before the buckling load. In such a case, the yield condition is defined by the axial force N and the biaxial bending moments M as follows.

$$F = \sqrt{\left(\frac{M}{M_P}\right)^2} - \cos\left(\frac{\pi N}{2N_P}\right) = 0, \qquad M = \sqrt{M_y^2 + M_z^2} \tag{45}$$

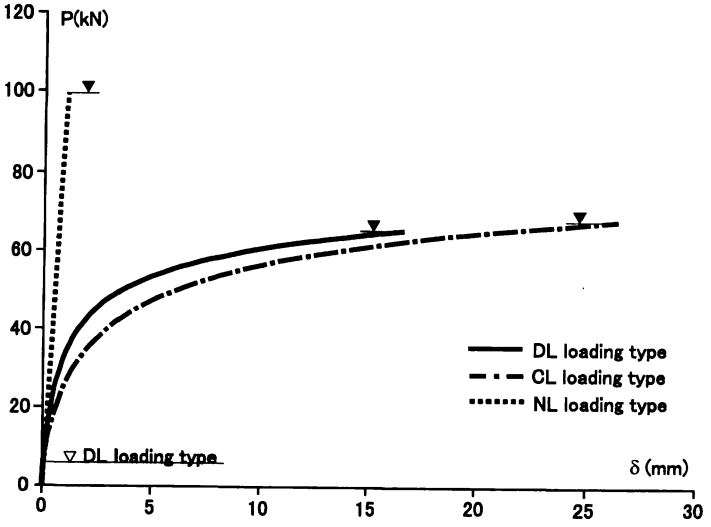

Fig.3 Total load – deflection relationships of 3 structural units

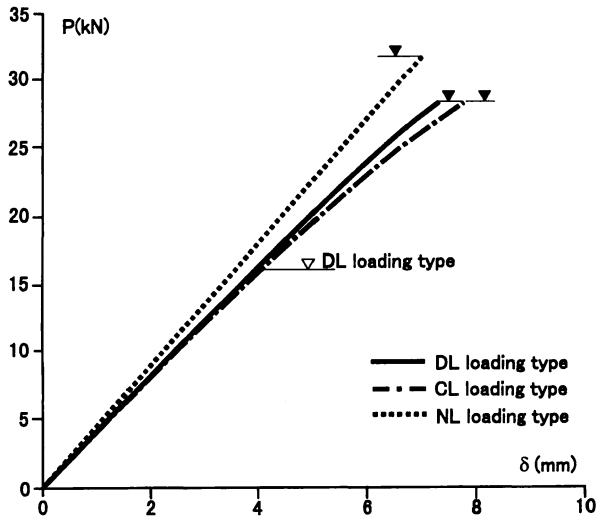

Fig.4 Total load – deflection relationships of 10 structural units

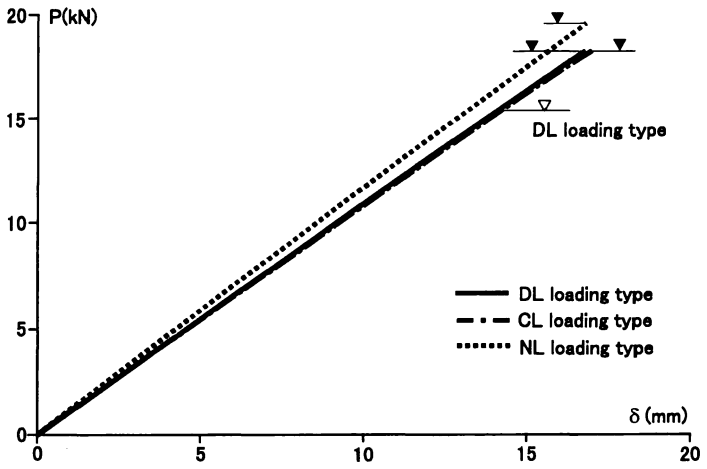

Fig.5 Total load – deflection relationships of 16 structural units

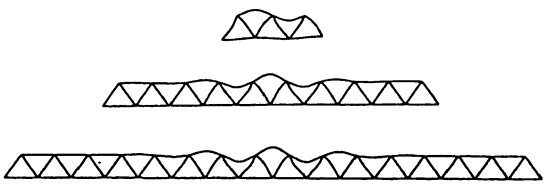

Fig.6 Elastic buckling mode of DL loading type

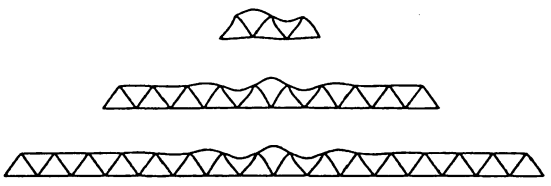

Fig.7 Elastic buckling mode of NL loading type

Table 3 Elastic buckling load

Loading type	Number of structural units		
	3	10	16
NL	99.87	31.92	19.50
DL	65.19 (65.3%)	28.44 (89.1%)	18.21 (93.4%)
CL	67.80 (67.9%)	28.44 (89.1%)	18.21 (93.4%)

( ) denotes the ratio to NL loading type. (kN)

The obtained elastic buckling loads are shown in Table 3. In the figures, the two elastic buckling loads by the present equations and the conventional matrix method are similar to each other at the each structural unit. However, the deformation of the conventional matrix method (CL type) ,where the distributed loads are considered as concentrated loads on additional nodes of a member, is larger than that of the present equations (DL type). The ratio between the two values of deformations is about 1.5 times for the 3 structural unit beam. The deformation of CL type is about 10 % higher than DL type for the 10 structural unit beam. For the 16 structural unit beam, the deformations of the two method are almost equal to each other. It may be caused by the reason that the geometrical nonlinear effect of members becomes relatively smaller on the geometrical nonlinearity of the whole structure. Then, it can be said that the differences of deformations depend upon the number of additional nodes of members. The each buckling mode shown in Figs.6 and 7 is member buckling that appears in the middle of beam.

The computing time of the conventional matrix method is about 9 times of the present method for the 3 structural unit beam and about 4 times for 10 or 16 structural unit beams. The present method can save the computing time and core storage.

Secondly, the effect of distributed load is considered by comparing the two results of NL and DL loading type. For the 3 structural unit beam, the load-deformation relationships by the distributed loads show strong nonlinearity and the elastic buckling load is about 35% smaller than NL loading type. The elastic buckling load of DL loading type is about 10% , 7% smaller than NL loading type at the 10, 16 structural unit case, respectively. Then it can be said that the reduction of elastic buckling load is relatively small while the number of structural units is large at the present model. Furthermore, when the material shown in Table 1 is used, the yield of members may be reached before an elastic buckling load. The initial yield load is about 10% of the elastic buckling load at the 3 structural unit beam, about 57% at the 10 unit case and 85% at the 16 unit case, respectively. However, this fact may not be always disadvantageous in practical design, that is, if the number of structural units is small, it may be sufficient for a designer to make the stiffness of members larger.

Model Experiment

Some model experiments were carried out in order to confirm the new tangent stiffness equations and make clear the buckling behaviour of latticed beam which is subjected to a laterally distributed load. The test model is shown in Fig.8. The test models consist of tubular brass members (φ5.0×t0.8 mm)and brass ball joints (φ15.9 mm) connected by steel bolts as shown in Fig.9. Table 4 shows the mechanical properties of members.

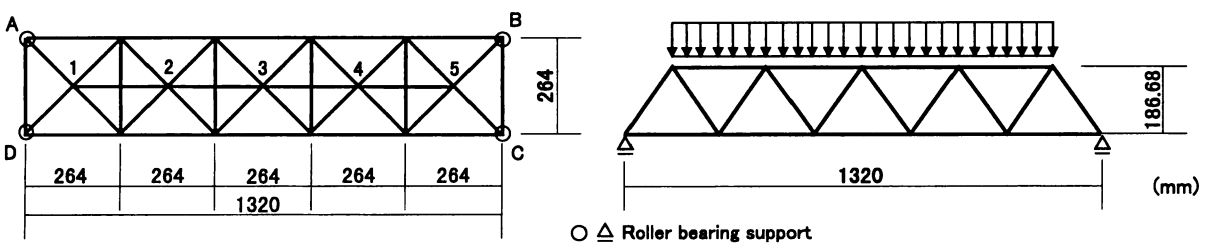

Fig.8 Latticed beam

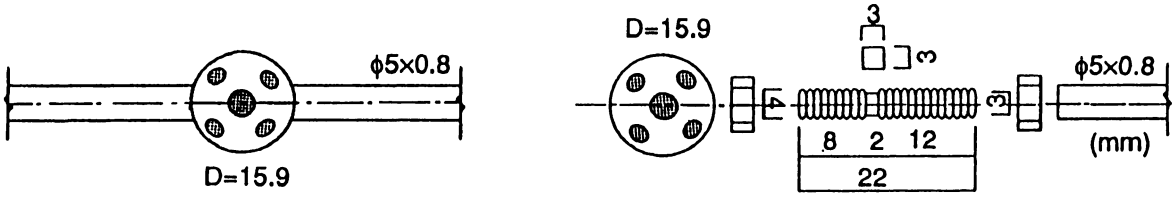

(a) Upper chord member (b) Bottom chord members

Fig.9 Jointing system

Table 4 Material strength and mechanical properties

(a) Brass Tubular Member	
Axial rigidity EA	1.11×10^{6} N
Flexural rigidity EI	2.87×10^{6} N mm^{2}
Yield bending moment M_P	6.37×10^{3} N mm
Yield tensile strength N_P	5.1×10^{3} N
(b) Joint	
Length of rigid end part $\lambda_j l$	11.9 mm
Rotational spring rigidity C_j	9.22×10^{4} N mm
Yield bending moment on connection M_{jP}	1.77×10^{3} N mm

In Fig.9(a), a continuos tubular member passes through all upper brass ball joints and is fixed by screw bolts in order to obtain rigid-jointed stiffness. The test models are roller supported at the both ends. The upper chord members are directly subjected to vertical loads ,as shown in Fig.10.

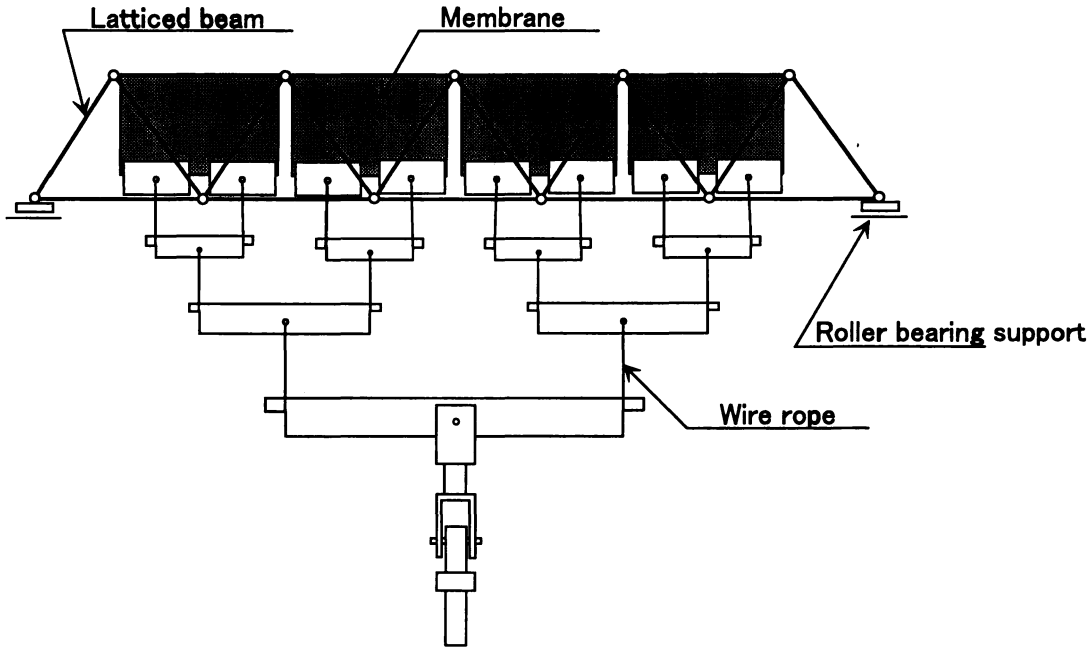

Fig.10 Distributed loading method

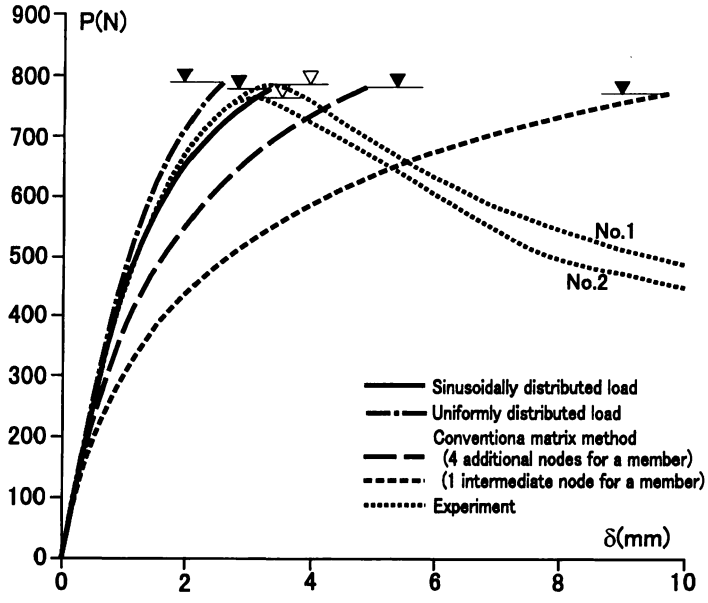

Fig.11 Total load-deflection relationships

The total load-deflection curves obtained by model experiments are shown in Fig.11 with numerical results. The vertical axis denotes the total load and the horizontal axis denotes the deflection of node 3 shown in Fig.8. The load-carrying capacity and the elastic buckling loads are shown in Table 5. The experimental curves are denoted as a dotted line.

The latticed structures gradually exhibited strong nonlinearity with the load increasing. The member buckling occurred at the peak load. After the peak load, the load-bearing capacity rapidly decreased. The deformation mode of a beam before the peak load is shown in Fig.12 and the residual deformations after the experiments are shown in Fig.13. In Fig.11, the upper chord members were bent in the vertical direction by the distributed loads. However at the peak load, the upper chord members buckled in the horizontal direction. It can be seen by the residual deformations shown in Fig.13.

The elastic buckling loads have been estimated by the present equations at the two distributed loading cases. In the numerical analyses, the member model is the one consisting of a uniform member, rigid end parts, and rotational springs for the bolted jointing system [6]. In Fig.11, the numerical result of a sinusoidally distributed load is denoted as a solid line, that of a uniformly distributed load is denoted as a dashed and dotted line. The elastic buckling load of each loading case is almost equal to each other.

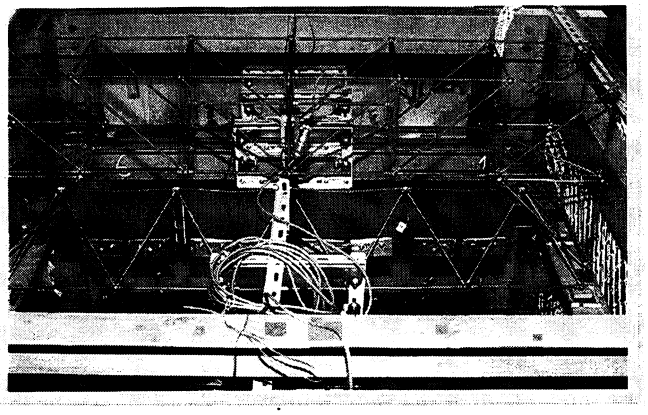

Fig.12 Deformation mode appearing before the peak load

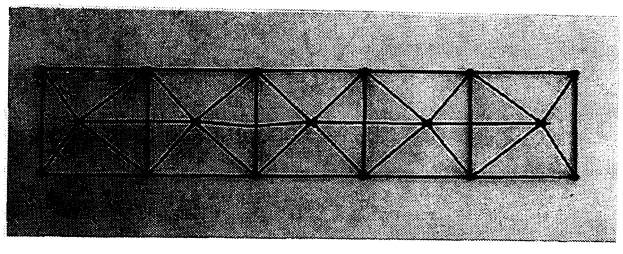

(a) No.1

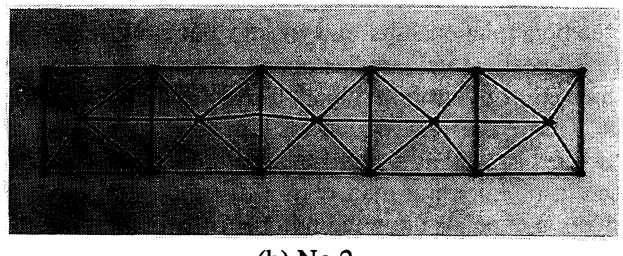

(b) No.2

Fig. 13 Residual deformation

Table 5 Load-carrying capacity and theoretical elastic buckling load

Experimental results (kN)		
Load-carrying capacity	No.1	782.8
	No.2	763.1
	Mean value	773.0(1±0.013)
Theoretical results (kN)		
Elastic buckling load of uniformly distributed load		785.3 (102%)
Elastic buckling load of sinusoidally distributed load		777.9 (101%)
Elastic buckling load by the conventional matrix method (4 additional nodes / a member)		780.0 (101%)
Elastic buckling load by the conventional matrix method (one intermediate node / a member)		772.8 (100%)

However, the deflections of a sinusoidally loaded case are larger than the uniform load. The experimental curves are relatively close to the curve of the sinusoidally distributed load case. During the experiments (see Fig.12), when the flexural deformation of upper chord members became larger, some wrinkles appeared in the loading sheets and the shape of distributed load seemed to be close to a sinusoidal shape.
The elastic buckling mode obtained by the numerical analysis is shown in Fig.14. The theoretical buckling mode corresponds with the experimental mode. Furthermore in Fig.11, the results by the conventional matrix method are shown. The long dashed line represents the curves of four additional nodes per a member and the short dashed line represents that of one intermediate additional node per a member. The distributed load is considered as a concentrated load acting on the additional nodes. The conventional matrix method has estimated a buckling load with a sufficient accuracy, however had a large tolerance in the estimation of deflection.

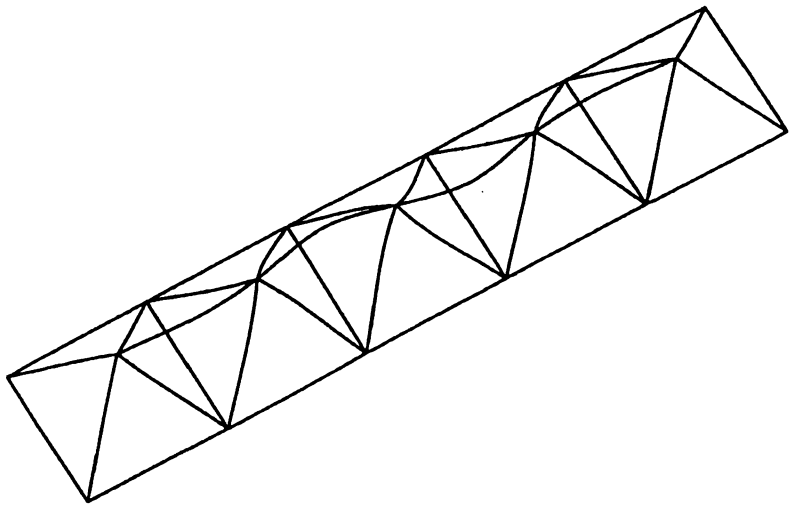

Fig.14 Theoretical elastic buckling mode (Sinusoidally distributed load)

Summary and Conclusions

Tangent stiffness equations of a beam-column which is subjected to sinusoidally or uniformly distributed lateral loads have been presented. Numerical study is carried out with the equations in order to investigate the load-deflection relationships and elastic buckling loads of parallel-chord latticed beam. The buckling behaviour of latticed beam structures has been theoretically and experimentally made clear, while the upper chord members are subjected to a distributed load. The following conclusions of the present work have been obtained:
The use of the new equations can lead to a good efficiency of estimating equilibrium paths of space frame structures as well as a significant savings in the core storage and computing time in the analysis.
The elastic buckling load with a distributed member load is smaller than the only nodal load case, however the reduction depends upon the number of structural units.
As for the present latticed beam with a vertical distributed load, the direction of member buckling mode is in horizontal plane, although the loading direction is vertical.

Appendix: Series expressions

The functions r_{uy}, b_{uy}, b'_{uy} of a uniform distributed load case become infinite at P_{ny}=0 and the functions r_{sy}, b_{sy}, b'_{sy} of a sinusoidal distributed load case also become infinite at P_{ny}=1. Then the following series expression have to be used.

$$r_{uy} = \frac{q_{ny} EI_y}{l}\left(10.335425 + 10.200655 P_{ny} + 10.187496 P_{ny}^2\right) \tag{46}$$

$$b_{uy3} = q_{ny}\left(1.722571\times10^{-1} + 8.095759\times10^{-2} P_{ny} + 2.996322\times10^{-2} P_{ny}^2\right) \tag{47}$$

$$b_{uy4} = q_{ny}^2\left(2.543357\times10^{-1} + 1.255096\times10^{-1} P_{ny} + 4.692159\times10^{-2} P_{ny}^2\right) \tag{48}$$

$$b'_{uy3} = q_{ny}\left(8.095758\times10^{-2} + 5.992645\times10^{-2} P_{ny} + 2.987123\times10^{-2} P_{ny}^2\right) \tag{49}$$

$$b'_{uy4} = q_{ny}^2\left(1.255097\times10^{-1} + 9.384325\times10^{-2} P_{ny} + 4.688637\times10^{-2} P_{ny}^2\right) \tag{50}$$

$$r_{sy} = \frac{q_{ny} EI_y}{l}\left(7.751569 + 1.233701 dZ_y + 4.496145\times10^{-1} dZ_y^2\right) \tag{51}$$

$$b_{sy3} = q_{ny}\left(1.963495\times10^{-1} + 8.061677\times10^{-2} dZ_y + 3.834705\times10^{-2} dZ_y^2\right) \tag{52}$$

$$b_{sy4} = q_{ny}^2\left(1.989139\times10^{-1} + 8.394592\times10^{-2} dZ_y + 4.005274\times10^{-2} dZ_y^2\right) \tag{53}$$

$$b'_{sy3} = q_{ny}\left(1.266214\times10^{-1} + 8.016471\times10^{-2} dZ_y + 4.674284\times10^{-2} dZ_y^2\right) \tag{54}$$

$$b'_{sy4} = q_{ny}^2\left(1.199180\times10^{-1} + 9.145578\times10^{-2} dZ_y + 4.590451\times10^{-2} dZ_y^2\right) \tag{55}$$

in which $dZ_y = l\sqrt{|N|/EI_y} - \pi$

References

1)L. Bognar and B.G. Strauber, "Load-Shortening Relationships for Bars", Journal of Structural Engineering, ASCE, Vol.115, No.7, pp.1711-1725 (1989)

2)R.E. McConnel, "Force Deformation Equations for Initially Curved Laterally Loaded Beam Columns", Journal of Structural Mechanics, ASCE, Vol.118, No.7, pp.1287-1302 (1992)

3)R.K. Livesley, "Matrix Methods of Structural Analysis", published by Pergamon Press, pp.233-234 (1964)

4)S.A. Saafan, "Nonlinear Behavior of Structural Plane Frames", Journal of the Structural Division, ASCE, Vol.89, No.4, pp.557-579 (1963)

5)C. Oran, "Tangent Stiffness in Space Frame", Journal of the Structural Division, ASCE, Vol.99, No.ST6, pp.987-1001 (1973)

6)T. Saka and Y. Taniguchi, "Effective Strength of Square-and-Diagonal Double-Layer Grid", Journal of Structural enginnering, ASCE, Vol.118, No.1, pp.52-72 (1992)